Pergamon

Int. J. Solids Structures Vol. 32, No. 5, pp. 647–663, 1995

0020-7683/95 $9.50 + .00

0020-7683(94)00143-X

FREE VIBRATIONS OF A ROTATING MULTI-LAYERED CYLINDRICAL SHELL

K. Y. LAM and C. T. LOY
Department of Mechanical and Production Engineering, National University of Singapore, 10 Kent Ridge Crescent, Singapore 0511

(*Received* 24 *November* 1993; *in revised form* 12 *May* 1994)

Abstract—In this paper parametric studies on the frequency properties of a rotating multi-layered cylindrical shell are undertaken. The equations of motion for the rotating multi-layered shell, which consider the effects of centrifugal, Coriolis and the initial hoop tension, are formulated using Love's first approximation theory. The analysis is carried out using closed-form solutions for the simply supported cylindrical shell. Results are presented for the frequency characteristics at different modes, geometric properties and different layered configurations of the rotating cylindrical shell. Effects of centrifugal and Coriolis influence on the frequencies and vibratory displacement are also considered. The present method is found to be accurate when compared with results available in the literature.

INTRODUCTION

The rotating cylindrical shell, which has a wide range of engineering applications such as gas turbines, locomotive engines, electric motors and rotor systems, was first studied more than a century ago. However, when compared with the stationary shell, the rotating shell is still very much less studied. A study of the free vibrations of a rotating cylindrical shell is therefore essential to the understanding of rotating structures.

The earliest recorded work on rotating cylindrical shells was by Bryan (1890) in which the free vibration of a rotating cylindrical shell was considered and the phenomenon of travelling modes was also discovered. Early works on rotating shells included the study of the Coriolis effect on the free vibration by Di Taranto and Lessen (1964) and Srinivasan and Lauterbach (1971) for infinitely long rotating shells and by Zohar and Aboudi (1973) for finite length rotating shells. Other works included the study of long rotating cylinders subjected to prestresses by Padovan (1973) and the study of vibrations and buckling of rotating anisotropic shells by Padovan (1975a). Cylindrical shells undergoing rotation and subjected to a radial excitation have been considered by Fox and Hardie (1985). In the more recent works, the free vibrations of rotating composite shells have been studied by Rand and Stavsky (1991) and a finite element analysis for rotating shells has been undertaken by Chen *et al.* (1993).

In most of these papers, the rotating shells considered were for a single-layered type of shells with the exception of Padovan (1975b), where multi-layered cylinders were studied. Furthermore, usually not enough parametric studies were carried out to understand the frequency properties of a rotating cylinder.

In this paper, parametric studies on the frequency properties were therefore undertaken for a rotating multi-layered cylindrical shell. The objective was to investigate and understand the frequency characteristics of a rotating multi-layered cylindrical shell, which are very often more useful than the single-layered type of shells because of the enhancement and improvement in the mechanical properties which the layering provides. The equations of motion, which take into account the effects of centrifugal, Coriolis and initial hoop tension, were formulated using Love's first approximation theory. The analysis was carried out using closed-form solutions for simply supported multi-layered cylindrical shells. In its present formulation, the analysis is valid for an arbitrarily layered cylindrical shell with different material properties and with different layered configurations. The present formulation can also be extended to include other boundary conditions using a solution method presented by Rand and Stavsky (1991).

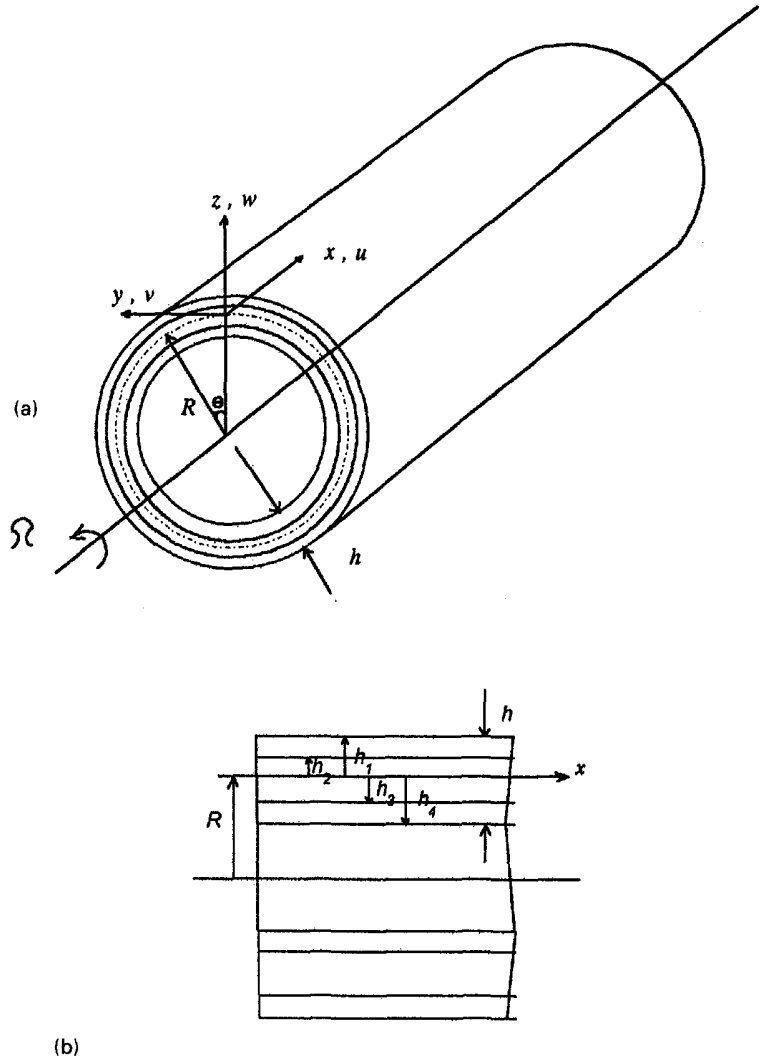

Fig. 1. (a) Geometry of a multi-layered cylindrical shell; (b) cross-sectional view of a multi-layered cylindrical shell.

In the parametric studies undertaken, results are presented for a three-layered cylindrical shell. The parametric studies carried out included the effects of centrifugal and Coriolis influence, the variations of natural frequencies with the rotating speeds and the modes of vibration, the influence of geometric properties and layered configurations on the natural frequencies and the influence of rotation on the vibratory displacements. The present analysis has been examined by comparing results with those in the literature for a stationary and a very long rotating cylindrical shell. In both cases, very good agreement was observed.

THEORETICAL FORMULATION

Figure 1(a) shows the nomenclature for a multi-layered cylindrical shell rotating about its horizontal axis at an angular velocity Ω, where L is the length, h is the thickness and R is the radius. The reference surface of the shell is taken to be at its middle surface where an orthogonal co-ordinate system (x, y, z) is fixed. The deformations of the cylinder are defined by u, v and w in the x, y and z directions, respectively.

The equations of motion for a rotating cylindrical shell can be written as

$$L_x(u,v,w)-\rho_t\frac{\partial^2 u}{\partial t^2}=0$$

$$L_y(u,v,w)-\rho_t\left(\frac{\partial^2 v}{\partial t^2}+2\Omega\frac{\partial w}{\partial t}-\Omega^2 v\right)=0$$

$$L_z(u,v,w)-\rho_t\left(\frac{\partial^2 w}{\partial t^2}-2\Omega\frac{\partial v}{\partial t}-\Omega^2 w\right)=0 \tag{1}$$

where

$$L_x=\frac{\partial N_x}{\partial x}+\frac{1}{R}\frac{\partial N_{x\theta}}{\partial\theta}+\tilde{N}_\theta\left(\frac{1}{R^2}\frac{\partial^2 u}{\partial\theta^2}-\frac{1}{R}\frac{\partial w}{\partial x}\right) \tag{2}$$

$$L_y=\frac{\partial N_{x\theta}}{\partial x}+\frac{1}{R}\frac{\partial N_\theta}{\partial\theta}+\frac{1}{R}\frac{\partial M_{x\theta}}{\partial x}+\frac{1}{R^2}\frac{\partial M_\theta}{\partial\theta}+\frac{\tilde{N}_\theta}{R}\frac{\partial^2 u}{\partial\theta\,\partial x} \tag{3}$$

$$L_z=\frac{\partial^2 M_x}{\partial x^2}+\frac{2}{R}\frac{\partial^2 M_{x\theta}}{\partial\theta\,\partial x}+\frac{1}{R^2}\frac{\partial^2 M_\theta}{\partial\theta^2}-\frac{N_\theta}{R}+\frac{\tilde{N}_\theta}{R^2}\left(\frac{\partial^2 w}{\partial\theta^2}-\frac{\partial v}{\partial\theta}\right) \tag{4}$$

$$\rho_t=\int_{-h/2}^{h/2}\rho\,\mathrm{d}z \tag{5}$$

where ρ and ρ_t are the density and density per unit length, respectively. $\tilde{N}=\rho_t\Omega^2 r^2$ is defined as the initial hoop tension due to the centrifugal force, and N_j and M_j are the force and moment resultants defined as

$$(N_x,N_\theta,N_{x\theta})=\int_{-h/2}^{h/2}(\sigma_x,\sigma_\theta,\sigma_{x\theta})\,\mathrm{d}z \tag{6}$$

$$(M_x,M_\theta,M_{x\theta})=\int_{-h/2}^{h/2}(\sigma_x,\sigma_\theta,\sigma_{x\theta})z\,\mathrm{d}z. \tag{7}$$

For a thin cylindrical shell, the stresses defined in eqns (6) and (7) are defined by the two-dimensional Hooke's law,

$$\begin{pmatrix}\sigma_x\\ \sigma_\theta\\ \sigma_{x\theta}\end{pmatrix}=\begin{bmatrix}Q_{11} & Q_{12} & 0\\ Q_{12} & Q_{22} & 0\\ 0 & 0 & Q_{66}\end{bmatrix}\begin{pmatrix}e_x\\ e_\theta\\ e_{x\theta}\end{pmatrix}, \tag{8}$$

where the strain components in eqn (8) have been defined as linear functions of the thickness coordinate z following Love's first approximation theory (1952) as

$$\begin{aligned}e_x&=e_1+z\,k_1\\ e_\theta&=e_2+z\,k_2\\ e_{x\theta}&=\gamma+2\,z\,\tau\end{aligned} \tag{9}$$

where e_x, e_θ and $e_{x\theta}$ are, respectively, the strains in the axial and circumferential directions and the shear strain at a distance z from the reference surface. e_1, e_2 and γ are the reference

surface strains and k_1, k_2 and τ are the reference surface curvatures. Both the reference surface strains and curvatures are defined as

$$\{e_1, e_2, \gamma\} = \left\{u_{,x}, \frac{1}{R}(v_{,\theta} + w), v_{,x} + \frac{1}{R}u_{,\theta}\right\} \tag{10}$$

$$\{k_1, k_2, \tau\} = \left\{-w_{,xx}, \frac{1}{R^2}(-w_{,\theta\theta} + v_{,\theta}), \frac{1}{R}(-w_{,x\theta} + v_{,x})\right\} \tag{11}$$

where the subscripts $,x; ,xx; ,\theta; ,\theta\theta; ,x\theta$ indicate the partial derivatives with respect to these parameters.

By substituting eqn (9) into (8) and then substituting the resulting equation into eqns (6) and (7), the force and moment resultants can be obtained as

$$\begin{bmatrix} N_x \\ N_\theta \\ N_{x\theta} \\ M_x \\ M_\theta \\ M_{x\theta} \end{bmatrix} = \begin{bmatrix} A_{11} & A_{12} & 0 & B_{11} & B_{12} & 0 \\ A_{12} & A_{22} & 0 & B_{12} & B_{22} & 0 \\ 0 & 0 & A_{66} & 0 & 0 & B_{66} \\ B_{11} & B_{12} & 0 & D_{11} & D_{12} & 0 \\ B_{12} & B_{22} & 0 & D_{12} & D_{22} & 0 \\ 0 & 0 & B_{66} & 0 & 0 & D_{66} \end{bmatrix} \begin{bmatrix} e_1 \\ e_2 \\ \gamma \\ k_1 \\ k_2 \\ 2\tau \end{bmatrix} \tag{12}$$

where A_{ij}, B_{ij} and D_{ij} are the extensional, coupling and bending stiffnesses defined, respectively, as

$$(A_{ij}, B_{ij}, D_{ij}) = \int_{-h/2}^{h/2} Q_{ij}(1, z, z^2)\, dz. \tag{13}$$

For an arbitrarily layered shell, these stiffnesses can be re-written as

$$A_{ij} = \sum_{k=1}^{N_i} Q_{ij}^k (h_k - h_{k-1}) \tag{14}$$

$$B_{ij} = \frac{1}{2}\sum_{k=1}^{N_i} Q_{ij}^k (h_k^2 - h_{k-1}^2) \tag{15}$$

$$D_{ij} = \frac{1}{3}\sum_{k=1}^{N_i} Q_{ij}^k (h_k^3 - h_{k-1}^3) \tag{16}$$

where N_i denotes the number of layers and h_k and h_{k-1} denote the distances from the shell reference surface to the outer and inner surface of the kth layer as indicated in Fig. 1(b). For a thin shell, which is assumed to be in a state of plane stress, Q_{ij}^k are the reduced stiffnesses for the kth layer defined as

$$Q_{11}^k = \frac{E_k}{1 - \nu_k^2} \tag{17}$$

$$Q_{12}^k = \frac{E_k \nu_k}{1 - \nu_k^2} \tag{18}$$

$$Q_{22}^k = \frac{E_k}{1-\nu_k^2} \tag{19}$$

$$Q_{66}^k = \frac{E_k}{2(1+\nu_k)} \tag{20}$$

where E_k and ν_k are the Young's modulus and Poisson's ratio for the kth layer.

By substituting eqn (12), with substitutions from eqns (10) and (11), into eqn (1), eqn (1) can be written in a matrix form as

$$\begin{bmatrix} L_{11} & L_{12} & L_{13} \\ L_{21} & L_{22} & L_{23} \\ L_{31} & L_{32} & L_{33} \end{bmatrix} \begin{Bmatrix} u \\ v \\ w \end{Bmatrix} = \begin{Bmatrix} 0 \\ 0 \\ 0 \end{Bmatrix} \tag{21}$$

where L_{ij} $(i,j = 1,2,3)$ are the differential operators with respect to x and θ.

In the parametric studies, a simply supported cylindrical shell is considered. The simply supported boundary conditions at the two ends of the shell, $x = 0$ and L, are

$$v = w = N_x = M_x = 0. \tag{22}$$

For the simply supported–simply supported boundary conditions, the solution which satisfies the boundary conditions can be expressed in closed form as

$$u = U\cos\left(\frac{m\pi x}{L}\right)\cos(n\theta+\omega t)$$

$$v = V\sin\left(\frac{m\pi x}{L}\right)\sin(n\theta+\omega t)$$

$$w = W\sin\left(\frac{m\pi x}{L}\right)\cos(n\theta+\omega t). \tag{23}$$

Substituting eqn (23) into eqns (10) and (11) and substituting eqn (12), with resulting expressions from (10) and (11) together with eqns from (13) to (20), into eqn (1), eqn (1) can be written in a matrix form as

$$\begin{pmatrix} C_{11} & C_{12} & C_{13} \\ C_{21} & C_{22} & C_{23} \\ C_{31} & C_{32} & C_{33} \end{pmatrix} \begin{pmatrix} U \\ V \\ W \end{pmatrix} = \begin{pmatrix} 0 \\ 0 \\ 0 \end{pmatrix}. \tag{24}$$

The details of the coefficients C_{ij} $(i,j = 1,2,3)$ are given in the Appendix. To solve for the eigenvalues ω, the non-trivial solutions condition is imposed by setting the determinant of the characteristic matrix in eqn (24) to zero; the eigenvalues ω can then be obtained by using the Newton–Raphson procedure.

RESULTS AND DISCUSSION

To examine the present analysis, comparisons are made with a simply supported non-rotating cylindrical shell and a very long rotating cylindrical shell. The comparison with

Table 1. Comparison of frequency parameter $\omega' = \omega h(\sqrt{(\rho/G)})/\pi$ for a non-rotating cylindrical shell with simply supported boundary conditions ($m = 1$, $h/R = 0.06$, $\nu = 0.3$)

$m\pi R/L$	n	Bhimaraddi (1984)	Present
0.5π	1	0.01853	0.01853
	2	0.01090	0.01090
	3	0.00828	0.00831
	4	0.01011	0.01021
π	1	0.02781	0.02787
	2	0.02214	0.02219
	3	0.01818	0.01827
	4	0.01748	0.01766
2π	1	0.03692	0.03748
	2	0.03612	0.03674
	3	0.03566	0.03640
	4	0.03632	0.03726

Table 2. Comparison of frequency parameter $\omega^* = \omega R\sqrt{((1-\nu^2)\rho/E)}$ for a very long rotating cylindrical shell ($h/R = 0.002$, $\nu = 0.3$)

		Chen *et al.* (1993)		Present	
Ω (rev/s)	n	ω_b^*	ω_f^*	ω_b^*	ω_f^*
0.05	2	0.00167	0.00142	0.00169	0.00144
	3	0.00448	0.00429	0.00449	0.00431
	4	0.00848	0.00833	0.00850	0.00835
	5	0.01370	0.01353	0.01370	0.01355
0.1	2	0.00180	0.00130	0.00186	0.00136
	3	0.00457	0.00419	0.00464	0.00427
	4	0.00855	0.00826	0.00863	0.00833
	5	0.01371	0.01347	0.01379	0.01355

Subscripts b and f denote the backward and forward waves, respectively. From eqn (45) of Chen *et al.* (1993).

$$\omega_b = \frac{2n}{n^2+1}\Omega + \sqrt{\frac{n^2(n^2-1)^2}{n^2+1}\frac{Eh^2}{\rho(1-\nu^2)12r^2} + \frac{n^4+3}{(n^2+1)^2}\Omega^2}$$

$$\omega_f = \frac{2n}{n^2+1}\Omega - \sqrt{\frac{n^2(n^2-1)^2}{n^2+1}\frac{Eh^2}{\rho(1-\nu^2)12r^2} + \frac{n^4+3}{(n^2+1)^2}\Omega^2}.$$

the simply supported non-rotating shell is presented in Table 1, in which the frequency parameter $\omega' = \omega h(\sqrt{(\rho/G)})/\pi$ is compared for three different values of the parameter $m\pi R/L$ (0.5π, π and 2π) and for the parameter $h/R = 0.06$. The comparison with a very long rotating shell is presented in Table 2, in which the frequency parameter $\omega^* = R\omega\sqrt{((1-\nu^2)\rho/E)}$ is compared with the results obtained using eqn (45) in Chen *et al.* (1993) for two angular speeds of rotation ($\Omega = 0.05$ and 0.1 rev/s) and for the parameter $h/R = 0.002$. For both comparisons, a Poisson ratio $\nu = 0.3$ is used and in the frequency parameters defined above, E is the Young's modulus of elasticity, G is the shear modulus, ν is the Poisson's ratio, ρ is the density, h is the thickness, R is the radius and ω is the natural frequency of the shell. From the comparisons presented in the two tables, very good agreement is observed which indicates that the present analysis is accurate.

In the present paper, the free vibration characteristics for a rotating multi-layered cylindrical shell have been studied in greater depth. Four parametric studies are made in this paper. The first study is to investigate the influence of centrifugal and Coriolis effects on the natural frequencies of rotating cylindrical shells. The results are shown in Figs 2–4. In Fig. 2, the frequencies of the rotating shell have been normalized with respect to the corresponding natural frequencies f_0 for a non-rotating cylinder to show the significance of the rotational effects on the natural frequencies. The second study is to investigate the frequency characteristics for different geometric properties of the cylindrical shell. The results are shown in Figs 5–8. The third study is to investigate the influence of different layered configurations on the natural frequencies. For this study, three cylindrical shells

Table 3. Properties of materials for multi-layered cylindrical shells

Cylinder	Layer	h (mm)	E (N/m^2)	ν	ρ (kg/m^3)
I					
	Inner	$h_o/5$	4.8265×10^9	0.3	1314
	Middle	$3h_o/5$	2.0685×10^{11}	0.3	8053
	Outer	$h_o/5$	4.8265×10^9	0.3	1314
II					
	Inner	$3h_o/7$	4.8265×10^9	0.3	1314
	Middle	$h_o/7$	2.0685×10^{11}	0.3	8053
	Outer	$3h_o/7$	4.8265×10^9	0.3	1314
III					
	Inner	$h_o/3$	4.8265×10^9	0.3	1314
	Middle	$h_o/3$	2.0685×10^{11}	0.3	8053
	Outer	$h_o/3$	4.8265×10^9	0.3	1314

$h_o = 2$ mm.

with different layer thickness are considered. The three cylindrical shells which have three layers of construction are termed cylinder I, II and III to differentiate their different layered configurations. Cylinder I has a middle layer which is three times the thickness of the other two layers; cylinder II has a thin middle layer which is three times thinner than the other two layers; cylinder III has equal thickness for all the three layers. Their geometrical and material properties are given in Table 3. The results for this study are shown in Figs 9–11. The last study is to investigate the influence of the rotation on the vibratory displacement of the shell. The results are shown in Figs 12–14. For the four studies carried out, the first, second and fourth study involve cylinder I and the third study involves all three cylinders.

The free vibration solution for a rotating cylindrical shell is a function of the rotational speed. For a given rotational speed, the two smallest eigensolutions for each mode of the vibration, i.e. for each pair of the wave numbers (m, n) where m is the axial wave number and n is the circumferential wave number, consist of positive and negative eigenvalues. These two eigenvalues correspond to the natural frequencies for the backward and forward travelling waves or to the natural frequencies for positive and negative rotational speeds of the shell. The positive eigenvalue corresponding to the backward waves is due to a rotation $\Omega > 0$ and the negative eigenvalue corresponding to the forward waves is due to a rotation $\Omega < 0$. In the case of a stationary shell, these two eigenvalues are identical and the vibratory motion of the shell is a standing wave motion. However as the shell started to rotate, this standing wave motion is transformed, and, depending on the direction of rotation, backward or forward waves are present. Two rotational effects are introduced when the shell rotated; one is the centrifugal effect and the other is the Coriolis effect. These effects are found to have different influences on the frequency characteristics of the shell in the present study.

Figure 2 illustrates the different influences which centrifugal and Coriolis effects have on the natural frequencies of a rotating shell. The present study shows that, when both the centrifugal and Coriolis effects are present, the natural frequencies associated with the backward waves are found to increase monotonically with the rotational speed and for the forward waves, the natural frequencies decreased initially and then increased gradually with the rotational speed. When only the centrifugal effect is present, which is obtained by omitting the $2\Omega\omega$ term in the equations of motion, the natural frequencies for both the backward and forward waves are found to increase monotonically and there is very little difference between the natural frequencies of the two waves. However, at low rotational speeds there is a slight difference in the frequencies but this difference diminishes when the rotational speed increases. These observations indicate that the influence of Coriolis and centrifugal effects on the natural frequencies are different and the Coriolis effect is the major factor causing the difference in the natural frequencies between the forward and backward waves or the bifurcations of natural frequencies. From the normalized frequencies, the significance of the rotation influence on the natural frequencies is also clearly brought out. Finally, it is concluded that both centrifugal and Coriolis effects have significant influence

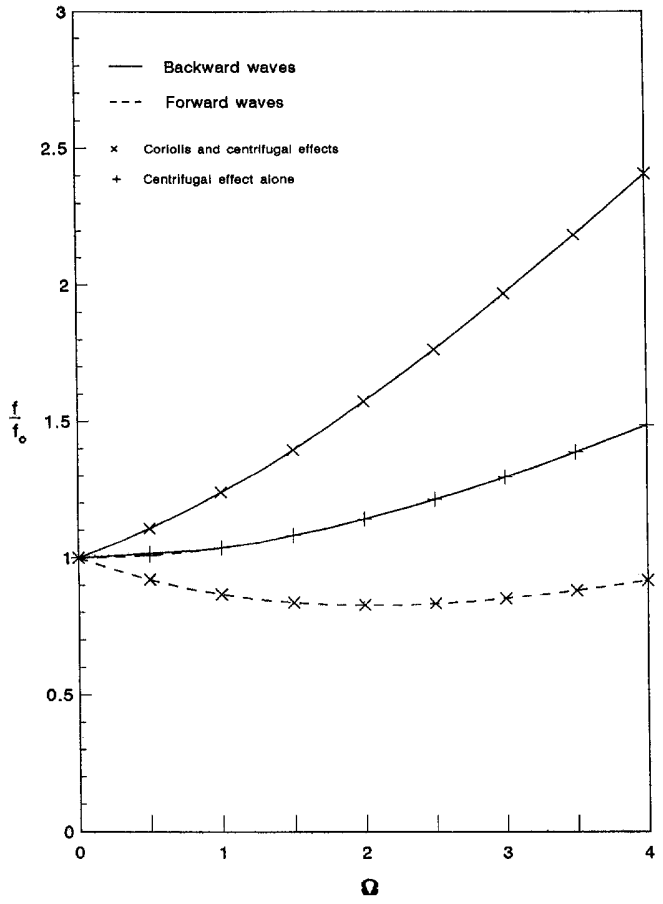

Fig. 2. Normalized natural frequency f/f_0 as a function of rotating speed Ω (rps) for a simply supported rotating multi-layered cylindrical shell ($m = 1$, $n = 2$, $h/R = 0.002$, $L/R = 20$).

on the natural frequencies and that these effects are important and should be considered when rotation is present.

Figure 3 illustrates the effect of the rotational speed on the frequency characteristics of a rotating shell. In the figure the frequency curves for the case of $\Omega = 0$, 1 and 4 rps (rps = revolutions per second or Hz) are shown. The general frequency characteristic of a rotating shell is similar to that of a stationary shell, i.e. the natural frequencies of both the backward and forward waves first decrease with the wave numbers and then increase. The natural frequencies of the backward waves are greater than those for a stationary shell, and for the forward waves, the natural frequencies are lower before the fundamental frequency for the stationary shell is attained and are always greater after the fundamental frequency has been attained. For any rotational speed, the difference between the natural frequencies of the forward and backward waves is always larger at a small circumferential wave number than at a big circumferential wave number, and this difference diminishes as the circumferential wave number becomes bigger. At small rotational speed, the difference between the frequencies of the two waves is small compared to when the rotational speed is high. This indicates that the rotational effect is significant at high rotational speeds.

Figure 4 shows the frequency characteristics of a rotating shell at various modes (m, n) of vibration. The vibrational modes shown in the figure are (1,2), (1,4), (2,2) and (2,4). For these modes, the natural frequencies of the two waves increase monotonically with the rotational speeds, except for the forward waves of the mode (1,2) which decrease initially and then increase with the rotational speeds. All the frequencies are found to increase uniformly as the rotational speeds become bigger.

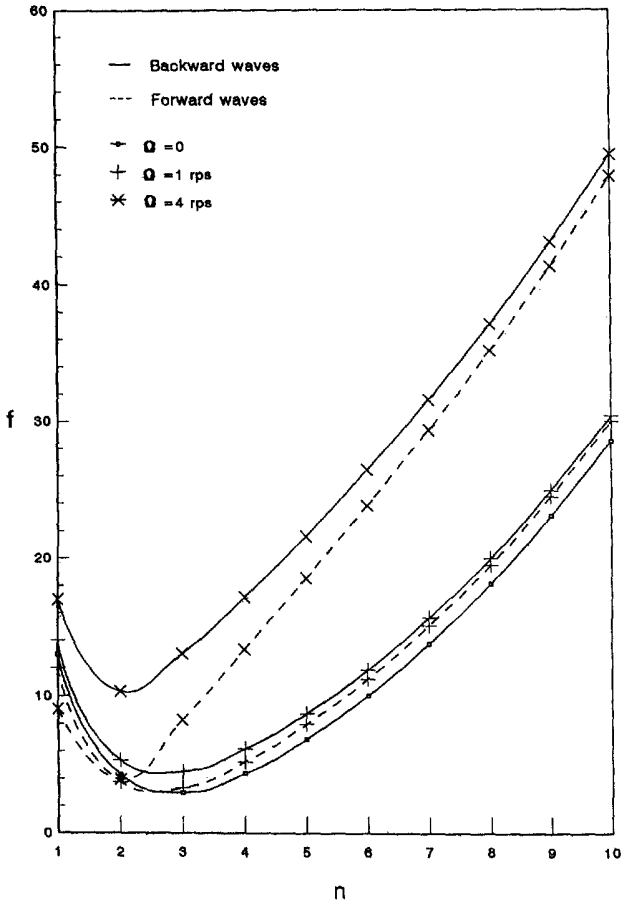

Fig. 3. Natural frequency f (Hz) as a function of circumferential wave number n for a simply supported rotating multi-layered cylindrical shell ($m = 1$, $h/R = 0.002$, $L/R = 20$).

Figure 5 shows the variation of the natural frequency with the rotational speed for different h/R ratios. The natural frequencies for the two waves increase with the h/R ratio for all rotational speeds. There is no obvious influence of the h/R ratio on the forward and the backward waves.

Figure 6 shows the variation of the natural frequency with the rotational speed for different L/R ratios. The natural frequencies of the two waves decrease with L/R ratios for all rotational speeds. There is no obvious influence of the L/R ratio on the forward waves and the backward waves.

Figures 7 and 8 show the variation of the fundamental frequency with L/R ratio for $\Omega = 0.5$ and 4 rps, respectively, and for the parameters $h/R = 0.002$ and 0.01. In both the figures, the fundamental frequencies for the two waves decrease with the L/R ratio. The fundamental frequencies for the forward and backward waves of a bigger h/R ratio are always larger than those of the corresponding waves of a smaller h/R ratio. For cylinder rotating at lower speed $\Omega = 0.5$ rps, bifurcation of natural frequencies for small L/R ratio is not significant. Bifurcation of natural frequencies becomes significant as the L/R ratio becomes larger. However for a cylinder rotating at the higher speed of $\Omega = 4$ rps, bifurcation of natural frequencies is relatively significant even at small L/R ratios. It also appears from the present study that the h/R ratio has little or no bifurcation effect on the natural frequencies. This can be noted from the apparently similar difference in natural frequency between the forward and backward waves at $h/R = 0.002$ and $h/R = 0.01$ for both speeds, $\Omega = 0.5$ and 4 rps.

Figures 9, 10 and 11 show the influence of the layered configuration on the natural frequency. Figure 9 shows the influence of the layered configuration on the variation of

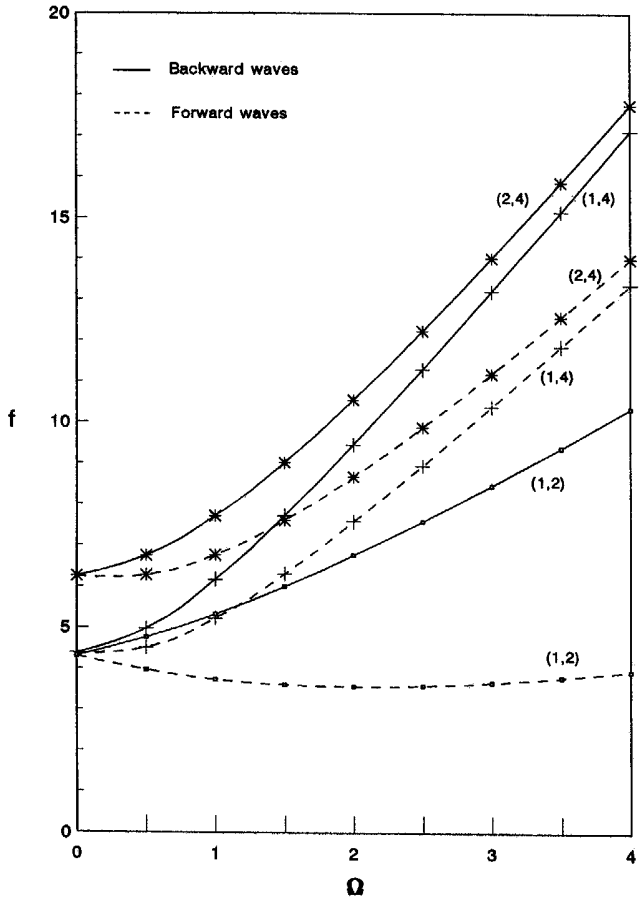

Fig. 4. Natural frequency f (Hz) at various modes of vibration as a function of rotating speed Ω (rps) for a simply supported rotating multi-layered cylindrical shell ($h/R = 0.002$, $L/R = 20$).

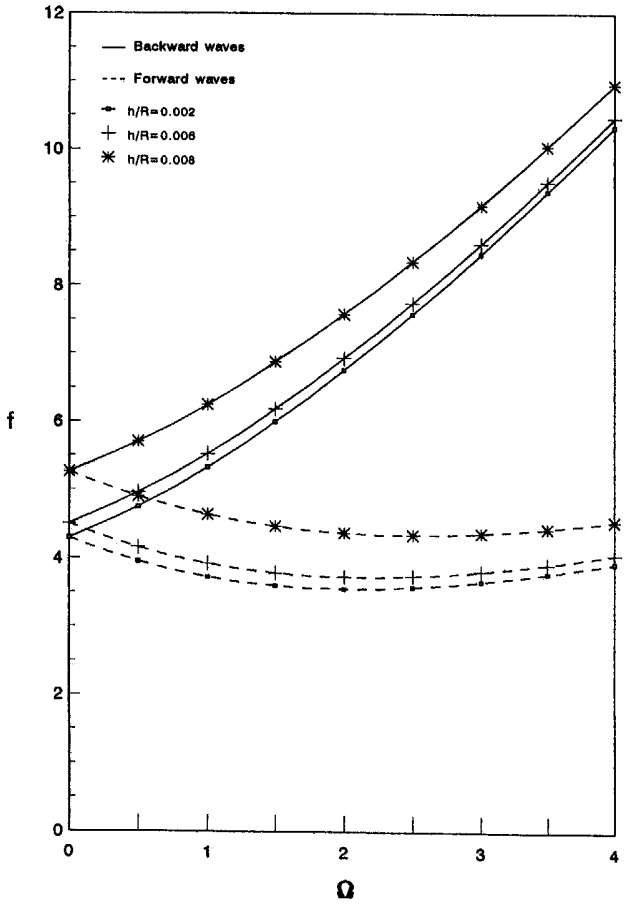

Fig. 5. Natural frequency f (Hz) as a function of rotating speed Ω (rps) at various h/R ratios for a simply supported rotating multi-layered cylindrical shell ($m = 1$, $n = 2$, $L/R = 20$).

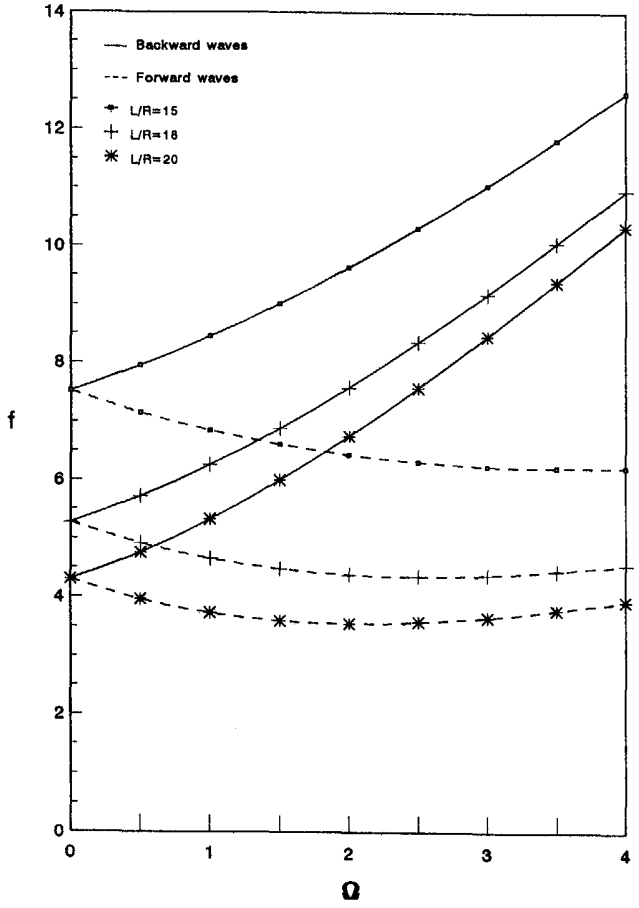

Fig. 6. Natural frequency f (Hz) as a function of rotating speed Ω (rps) at various L/R ratios for a simply supported rotating multi-layered cylindrical shell ($m = 1$, $n = 2$, $h/R = 0.002$).

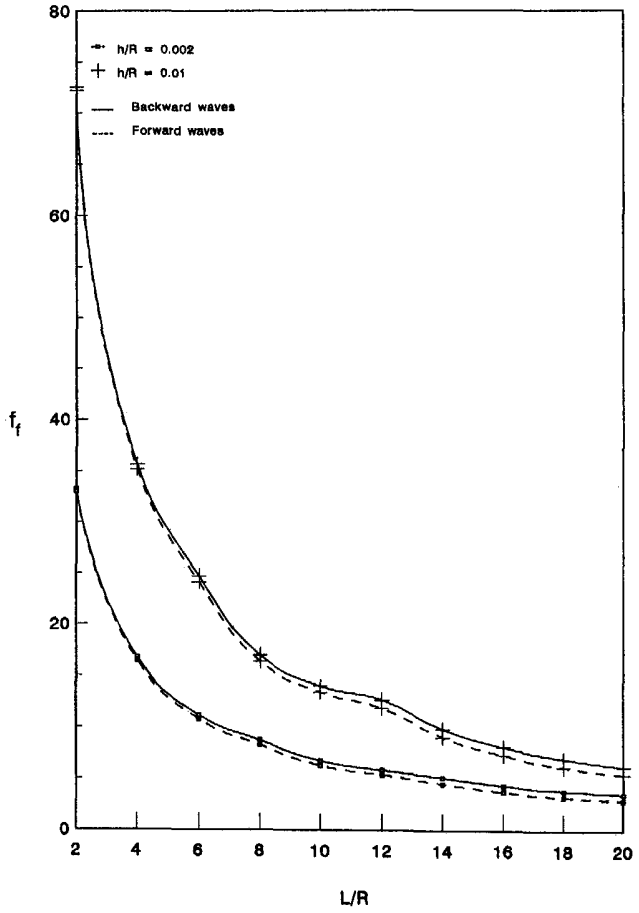

Fig. 7. Fundamental frequency f_f (Hz) as a function of L/R ratio for a simply supported rotating multi-layered cylindrical shell ($\Omega = 0.5$ rps).

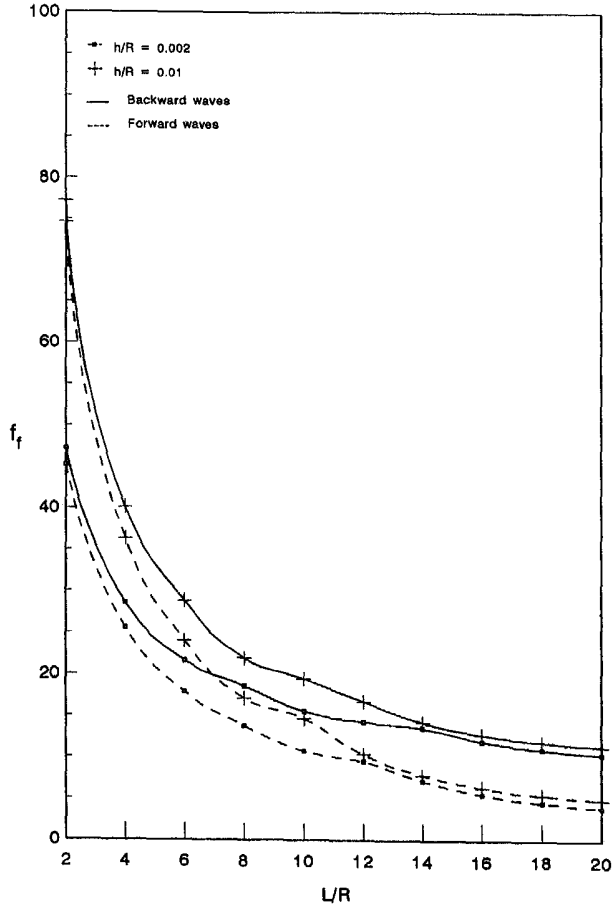

Fig. 8. Fundamental frequency f_f (Hz) as a function of L/R ratio for a simply supported rotating multi-layered cylindrical shell ($\Omega = 4$ rps).

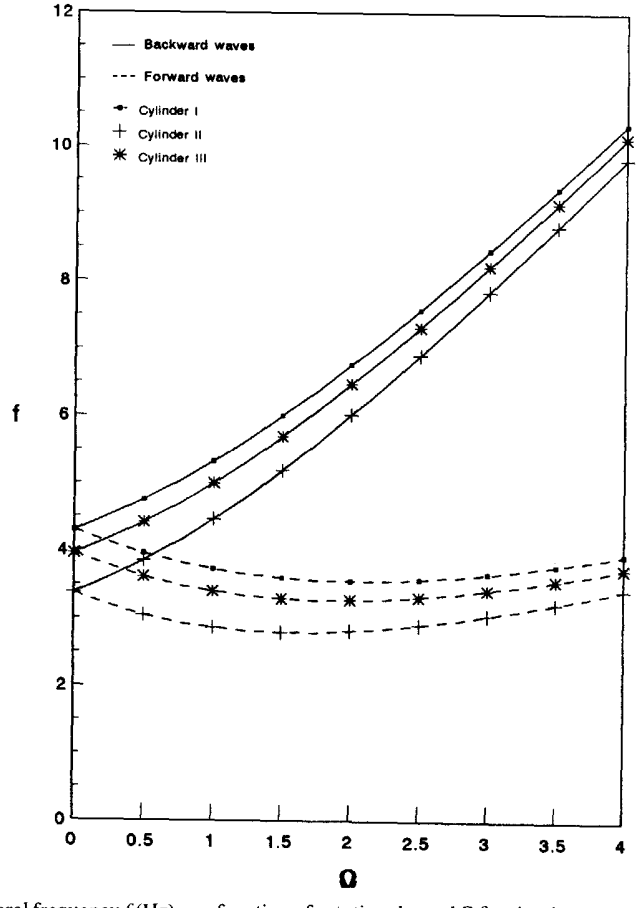

Fig. 9. Natural frequency f (Hz) as a function of rotational speed Ω for simply supported rotating cylinders with different layered configurations ($m = 1$, $n = 2$, $L/R = 20$, $h/R = 0.002$).

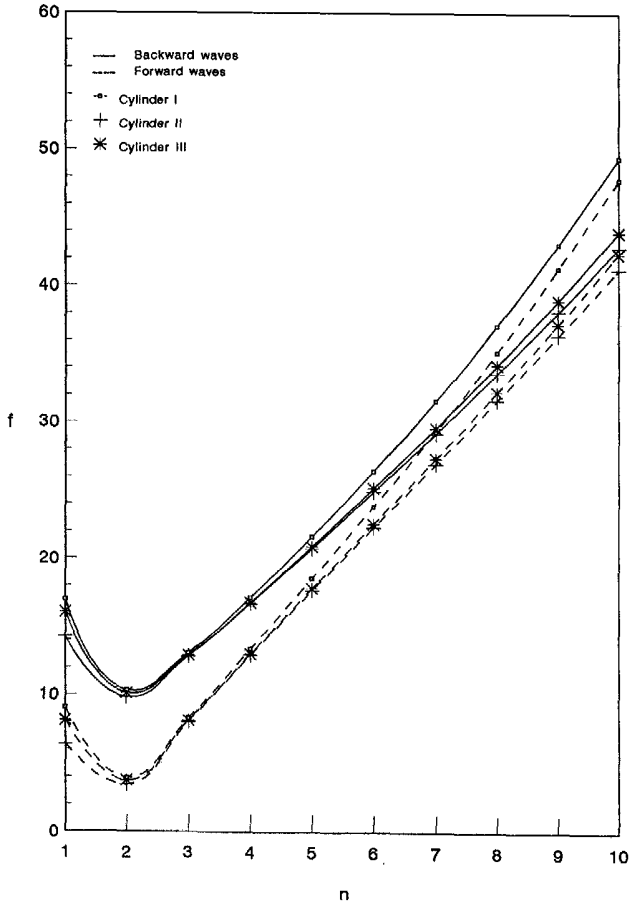

Fig. 10. Natural frequency f (Hz) as a function of circumferential wave number n for simply supported rotating cylinders with different layered configurations ($m = 1$, $\Omega = 4$ rps, $L/R = 20$, $h/R = 0.002$).

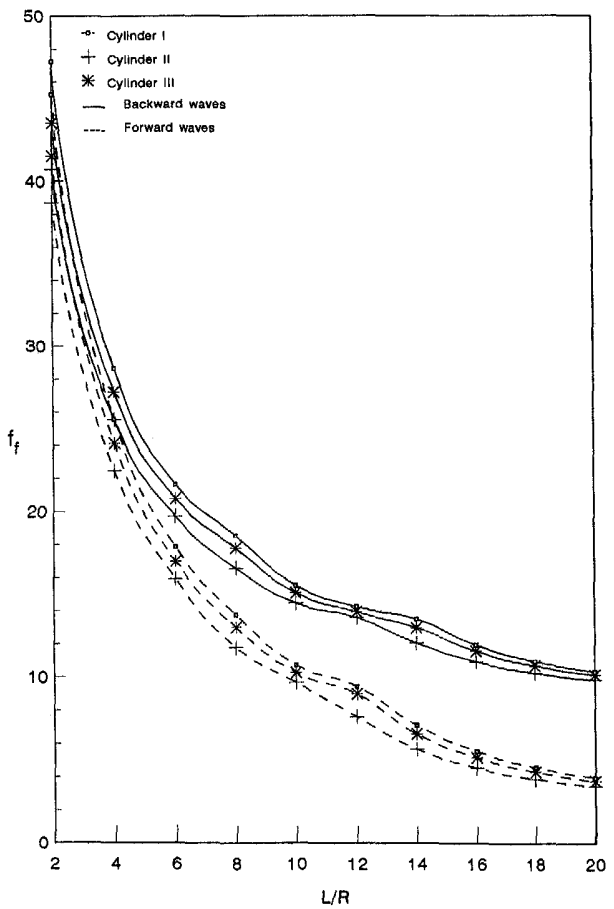

Fig. 11. Fundamental frequency f_f (Hz) as a function of L/R ratio for simply supported rotating cylinders with different configurations ($\Omega = 4$ rps).

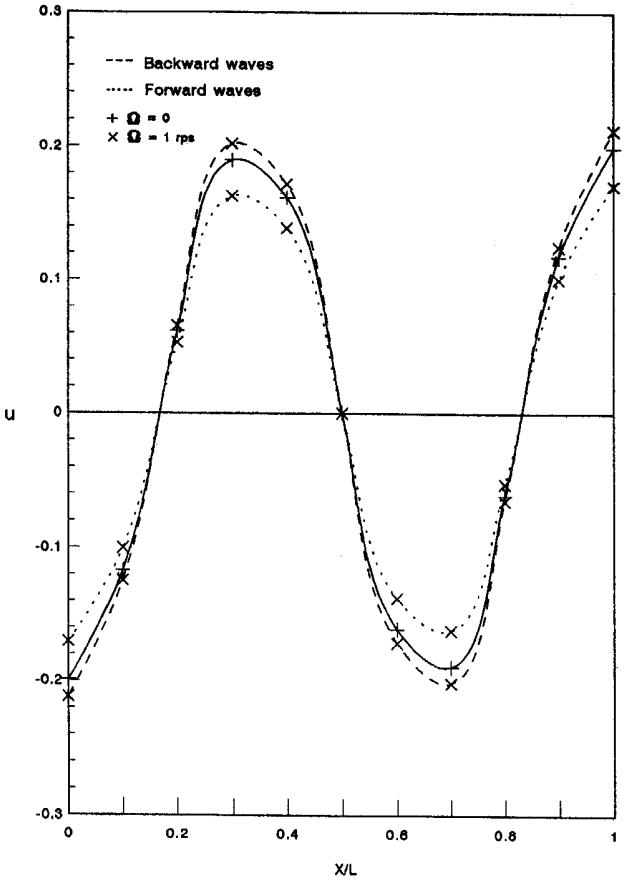

Fig. 12. Comparison of relative displacement u as a function of x/L for a simply supported rotating multi-layered cylindrical shell ($m = 3$, $n = 1$, $h/R = 0.002$, $L/R = 20$, $\theta = 10°$).

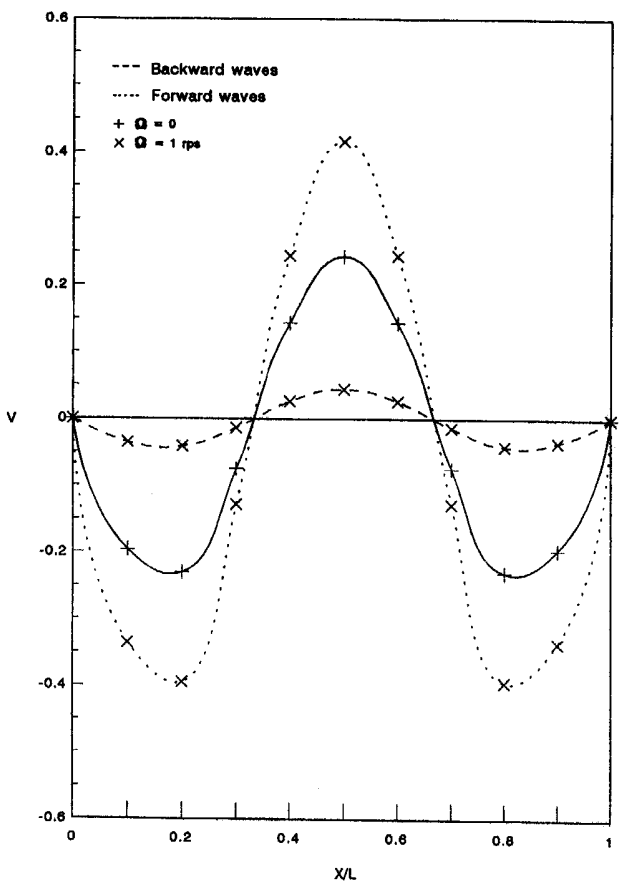

Fig. 13. Comparison of relative displacement v as a function of x/L for a simply supported rotating multi-layered cylindrical shell ($m = 3$, $n = 1$, $h/R = 0.002$, $L/R = 20$, $\theta = 10°$).

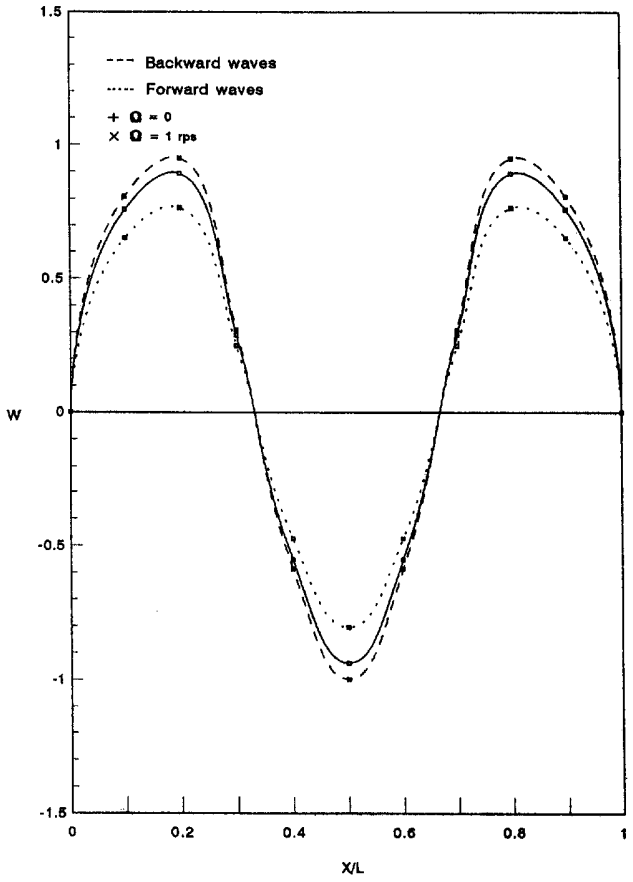

Fig. 14. Comparison of relative displacement w as a function of x/L for a simply supported rotating multi-layered cylindrical shell ($m = 3$, $n = 1$, $h/R = 0.002$, $L/R = 20$, $\theta = 10°$).

natural frequency with the rotational speed for cylinders I, II and III. The study shows that cylinder I, which has a thicker middle layer than the outer and inner layers, has higher natural frequencies for the forward and backward waves followed by cylinder III, which has all layers of equal thickness, and cylinder II, which has a thinner middle layer than the other two layers.

Figure 10 shows the influence of layered configuration on the variation of the natural frequency with the circumferential wave number. The natural frequencies for the forward and backward waves for the three cylinders first decrease and then increase with the circumferential wave numbers. Cylinder I has higher natural frequencies, followed by cylinder III and cylinder II.

Figure 11 shows the influence of layered configuration on the variation of the fundamental frequency with the L/R ratios. For the three cylinders, the fundamental frequencies for the forward and backward waves decrease with the L/R ratios. Cylinder I has higher fundamental frequencies, followed by cylinder III and cylinder II.

Figures 12–14 compare the relative displacements of cylinder I for $\Omega = 0$ and 1 rps. It is found that rotation has a significant influence on the vibratory displacement response of the cylinder, and the influence is most significant at places where the displacements are a maximum. Further examination also showed that the difference in the relative displacements between a stationary cylinder $\Omega = 0$ and that due to backward and forward waves at $\Omega = 1$ rps in the u direction are 6.4% and 14.3%, respectively. In the v direction, these differences are 82% and 71.2%, respectively and in the w direction, the differences are 6.4% and 14.2%, respectively. This indicates that the rotational motion on the vibratory displacement of the cylindrical shell is significant and the effect is also most prominent in the v direction.

The results show that rotational motion has a significant effect on both the frequencies and vibratory displacement of the shell, and these effects depend largely on the speed of rotation.

CONCLUSIONS

Parametric studies for the free vibrations of a thin rotating multi-layered cylindrical shell have been presented. Results on the influence of rotation on the frequency characteristics and vibratory displacements and the frequency characteristics at different modes of vibration, geometric properties and layered configurations are presented. Interesting insights are also shed in the course of the study. The present work can also be extended to study rotating composite laminated shells.

REFERENCES

Bhimaraddi, A. (1984). A higher order theory for free vibration analysis of circular cylindrical shells. *Int. J. Solids Structures* **20,** 623–630.

Bryan, G. H. (1890). On the beats in the vibration of revolving cylinder or bell. *Proc. Cambridge Phil. Soc.* **7,** 101–111.

Chen, Y., Zhao, H. B. and Shen, Z. P. (1993). Vibrations of high speed rotating shells with calculations for cylindrical shells. *J. Sound Vibr.* **160,** 137–160.

Di Taranto, R. A. and Lessen, M. (1964). Coriolis acceleration effect on the vibration of a rotating thin-walled circular cylinder. *J. Appl. Mech.* **31,** 700–701.

Fox, C. H. J. and Hardie, D. J. W. (1985). Harmonic response of rotating cylindrical shells. *J. Sound Vibr.* **115,** 253–274.

Love, A. E. H. (1952). *A Treatise on the Mathematical Theory of Elasticity*. Fourth edition. Cambridge University Press, Cambridge.

Padovan, J. (1973). Natural frequencies of rotating prestressed cylinders. *J. Sound Vibr.* **31,** 469–482.

Padovan, J. (1975a). Travelling waves vibrations and buckling of rotating anisotropic shells of revolution by finite elements. *Int. J. Solids Structures* **11,** 1367–1380.

Padovan, J. (1975b). Numerical analysis of asymmetric frequency and buckling eigenvalues of prestressed rotating anisotropic shells of revolution. *Computers Struct.* **5,** 145–154.

Rand, O. and Stavsky, Y. (1991). Free vibrations of spinning composite cylindrical shells. *Int. J. Solids Structures* **28,** 831–843.

Srinivasan, A. V. and Lauterbach, G. F. (1971). Travelling waves in rotating cylindrical shells. *J. Engng Industry* **93,** 1229–1232.

Zohar, A. and Aboudi, J. (1973). The free vibrations of thin circular finite rotating cylinder. *Int. J. Mech. Sci.* **15,** 269–278.

APPENDIX

The coefficients C_{ij} in the eqn (24) are defined as follows:

$$C_{11} = -\frac{A_{11}m^2\pi^2}{L^2} - \frac{A_{66}n^2}{R^2} - n^2\Omega^2\rho_t + \omega^2\rho_t \tag{A1}$$

$$C_{12} = \frac{B_{12}mn\pi}{LR^2} + \frac{2B_{66}mn\pi}{LR^2} + \frac{A_{12}mn\pi}{LR} + \frac{A_{66}mn\pi}{LR} \tag{A2}$$

$$C_{13} = \frac{B_{11}m^3\pi^3}{L^3} + \frac{B_{12}mn^2\pi}{LR^2} + \frac{2B_{66}mn^2\pi}{LR^2} + \frac{A_{12}m\pi}{LR} - \frac{m\Omega^2\pi R\rho_t}{L} \tag{A3}$$

$$C_{21} = \frac{B_{12}mn\pi}{LR^2} + \frac{B_{66}mn\pi}{LR^2} + \frac{A_{12}mn\pi}{LR} + \frac{A_{66}mn\pi}{LR} + \frac{mn\Omega^2\pi R\rho_t}{L} \tag{A4}$$

$$C_{22} = -\frac{A_{66}m^2\pi^2}{L^2} - \frac{D_{22}n^2}{R^4} - \frac{2B_{22}n^2}{R^3} - \frac{A_{22}n^2}{R^2} - \frac{2D_{66}m^2\pi^2}{L^2R^2} - \frac{3B_{66}m^2\pi^2}{L^2R} + \omega^2\rho_t + \Omega^2\rho_t \tag{A5}$$

$$C_{23} = -\frac{D_{22}n^3}{R^4} - \frac{B_{22}n}{R^3} - \frac{B_{22}n^3}{R^3} - \frac{A_{22}n}{R^2} - \frac{D_{12}m^2n\pi^2}{L^2R^2} - \frac{2D_{66}m^2n\pi^2}{L^2R^2} - \frac{B_{12}m^2n\pi^2}{L^2R} - \frac{2B_{66}m^2n\pi^2}{L^2R} + 2\omega\Omega\rho_t \tag{A6}$$

$$C_{31} = \frac{B_{11}m^3\pi^3}{L^3} + \frac{B_{12}mn^2\pi}{LR^2} + \frac{2B_{66}mn^2\pi}{LR^2} + \frac{A_{12}m\pi}{LR} \tag{A7}$$

$$C_{32} = -\frac{D_{22}n^3}{R^4} - \frac{B_{22}n}{R^3} - \frac{B_{22}n^3}{R^3} - \frac{A_{22}n}{R^2} - \frac{D_{12}m^2n\pi^2}{L^2R^2} - \frac{4D_{66}m^2n\pi^2}{L^2R^2}$$

$$- \frac{B_{12}m^2n\pi^2}{L^2R} - \frac{2B_{66}m^2n\pi^2}{L^2R} + 2\omega\Omega\rho_t - n\Omega^2\rho_t \quad \text{(A8)}$$

$$C_{33} = -\frac{D_{11}m^4\pi^4}{L^4} - \frac{D_{22}n^4}{R^4} - \frac{2B_{22}n^2}{R^3} - \frac{A_{22}}{R^2} - \frac{2D_{12}m^2n^2\pi^2}{L^2R^2} - \frac{4D_{66}m^2n^2\pi^2}{L^2R^2}$$

$$- \frac{2B_{12}m^2\pi^2}{L^2R} + \Omega^2\rho_t R + \omega^2\rho_t - n^2\Omega^2\rho_t. \quad \text{(A9)}$$